Photocurrent Spectrum and Photoelectron Counts Produced by a Gas Laser*

CHARLES FREED
Lincoln Laboratory,† Massachusetts Institute of Technology, Lexington, Massachusetts

AND

HERMANN A. HAUS
Department of Electrical Engineering and Research Laboratory of Electronics,† Massachusetts Institute of Technology, Cambridge, Massachusetts

(Received 4 August 1965)

The anode-current spectrum of a photomultiplier illuminated by light of time-varying intensity is obtained theoretically. The moments of the photoelectron counts under the same conditions are derived. The expressions are evaluated for the case of light emitted from a laser oscillator by using a semiclassical theory of the Van der Pol oscillator. The theoretical predictions are compared with experiments in which the spectrum of the photomultiplier was observed in the range 0–17 Mc/sec and counts were recorded for counting intervals in the range between 10^{-6} and 10^{-1} sec. The three lowest order factorial moments were evaluated as functions of T and compared with theory. The spectral data are used to predict the counting data and a comparison is made. The signal-to-noise ratio of the two types of experiments is evaluated and found to be comparable.

I. INTRODUCTION

WHEN a light source illuminates the photocathode of a photomultiplier, the current in the anode carries information about the intensity fluctuations of the light. This information can be extricated either by measuring the spectrum of the anode current or by performing counting experiments on the number of photoelectrons emitted within preset time intervals. Measurements of the intensity fluctuations of the light emitted from an optical maser can be used to probe the nature of the optical oscillations. In particular, it is possible to check experimentally whether the intensity fluctuations of an optical maser can be explained on the basis of the Van der Pol oscillator model of the optical maser.[1]

This paper presents a brief summary of the probability distribution for a compound Poisson process. This is the probability distribution of the electron count, within a time interval T, of a photomultiplier illuminated by light of time-varying intensity. From this distribution the factorial moments of the electron count are obtained. The connection with a quantum-mechanical analysis is established. Next, the expression for the spectrum of the photocurrent in the photomultiplier is derived. It is shown that the second factorial moment of the photoelectron counts within time intervals of sequentially varied duration T contains the same information as a measurement of the spectrum of the photomultiplier current. Thus far, no assumptions are made about the nature of the incident light. At this point in the development, the theory is applied to the case in which intensity fluctuations are those predicted by a semiclassical analysis of noise in the Van der Pol oscillator. Theoretical expressions are developed with only one parameter, the noise bandwidth, left to be determined experimentally. All other parameters can be evaluated from the known mirror reflectivity, spacing, etc.

Armstrong and Smith,[2] using the counting method, have reported measurements of the intensity fluctuations of a gallium arsenide laser. We now report measurements of the intensity fluctuations of He-Ne lasers at 6328 Å operating both below and above threshold.[3] These were made by using the spectral method, as well as the second factorial moment determined from the photoelectron count. The measurements are in good quantitative agreement with theory. Measurements of the third and fourth factorial moment of the photoelectron count are also reported and compared with the theory.

Finally, a summary of the signal-to-noise ratio of the spectral measurement and the counting measurement is presented; both measurements lead to comparable signal-to-noise ratios. The experiments reported here operated under very favorable conditions with regard to the theoretical signal-to-noise ratio limitations.

II. THEORY OF THE SPECTRAL MEASUREMENT AND THE PHOTOELECTRON COUNTING EXPERIMENT

When light of time-varying intensity impinges upon a photocathode, the probability of emission of a photoelectron varies with time. In the theory of photoemission, it is customary to assume that the probability $w(t)dt$ of emission of a photoelectron within the time in-

* This work was supported in part by the Joint Services Electronics Program under Contract DA36-039-AMC-03200(E).
† Operated with support from the U. S. Air Force.
[1] W. E. Lamb, Jr., Phys. Rev. 134, A1429 (1964).

[2] J. A. Armstrong and A. W. Smith, Phys. Rev. Letters 14, 68 (1965); Proceedings of the 1965 Physics of Quantum Electronics Conference (to be published).
[3] C. Freed and H. A. Haus, MIT Lincoln Laboratory, Solid State Res., Report No. 2, 1964 (unpublished); Appl. Phys. Letters 6, 85 (1965); Proceedings of the 1965 Physics of Quantum Electronics Conference (to be published).

crement dt is given[4] by

$$w(t)dt=(\varphi/h\nu)p(t)dt. \quad (1)$$

Here, φ is the quantum efficiency of the cathode, h is Planck's constant, ν is the frequency of the light, and $p(t)$ is the (short) time average of the light power over a few cycles of the optical frequency.

Starting with (1), and assuming that the probability of emission of a photoelectron within the time increment dt is independent of the emission within any other time increment, one finds[4] for the probability $W(n)$ of exactly n photoelectrons emitted within the time interval t, $t+T$,

$$W(n)=\frac{\beta^n}{n!}\left[\int_t^{t+T} p(t)dt\right]^n \exp\left(-\beta\int_t^{t+T} p(t)dt\right), \quad (2)$$

where

$$\beta=\varphi/h\nu.$$

This is a compound Poisson distribution. As in the case of the time-independent Poisson distribution, it is easy to show that the factorial moment of kth order is given by

$$\langle n(n-1)\cdots(n-k+1)\rangle_{\mathrm{av}}=\beta^k\left[\int_t^{t+T} p(t)dt\right]^k. \quad (3)$$

If the light itself is statistical in nature, an average must be taken with respect to the statistics of the light. Using a well-known identity for transforming the right-hand side of (3) into a k-dimensional integral, one obtains

$$\langle n(n-1)\cdots(n-k+1)\rangle_{\mathrm{av}}=\beta^k k!\int_t^{t+T} dt_k \times\int_t^{t_k} dt_{k-1}\cdots\int_t^{t_2} dt_1\langle p(t_1)\cdots p(t_{k-1})p(t_k)\rangle_{\mathrm{av}}. \quad (4)$$

Thus far we have treated the problem of photoelectron emission in a semiclassical way. Quantum analysis, as carried out by Kelley and Kleiner,[5] and Glauber,[5a] leads to an equation of the form (4), except that the correlation function of the power is to be replaced by the normal-ordered expression of the product of the field operators $E_\mu^{(-)}$ and $E_\mu^{(+)}$:

$$G^{(k)}=\mathrm{tr}[\rho E_{\mu_1}^{(-)}(\bar{x}_1,t_1)E_{\mu_2}^{(-)}(\bar{x}_2,t_2)\cdots E_{\mu_k}^{(-)}(\bar{x}_k,t_k) \times E_{\mu_k}^{(+)}(\bar{x}_k,t_k)\cdots E_{\mu_2}^{(+)}(\bar{x}_2,t_2)E_{\mu_1}^{(+)}(\bar{x}_1,t_1)], \quad (5)$$

and integrations over the surface of the photocathode have to be performed. Here ρ is the density matrix of the field, $t_1\leq t_2\cdots\leq t_k$, $G^{(k)}$ is Glauber's[6] correlation function of kth order. If $G^{(k)}$ is a slowly varying function of the $\bar{x}_i$ over the surface of the photocathode (as was the case in our experiment) the spatial arguments may be replaced by the coordinate of the center of the photocathode and integration over the spatial coordinates becomes multiplication by the area.

There is one special form of $G^{(k)}$ to which a more direct correspondence with the semiclassical expression (4) may be established[5,6]; this special form is obtained if one assumes that the incident light can be represented in Glauber's P representation[6] in terms of the free-space modes. Assuming for simplicity that the light is linearly polarized we have

$$G_{\mu\cdots\mu}^{(k)}(x,t_1\cdots x,t_k)=\int d^2\alpha P(\alpha)\mathcal{E}_\mu^{(-)}(\{\alpha\},\bar{x}_1,t_1) \times\mathcal{E}_\mu^{(+)}(\{\alpha\},\bar{x}_1,t_1)\cdots\mathcal{E}_\mu^{(-)}(\{\alpha\},\bar{x}_k,t_k) \times\mathcal{E}_\mu^{(+)}(\{\alpha\},\bar{x}_k,t_k), \quad (6)$$

where $\mathcal{E}_\mu^{(-)}$ and $\mathcal{E}_\mu^{(+)}$ are the eigenvalues of the eigenfunctions $|\{\alpha\}\rangle$ and $\langle\{\alpha\}|$.

$$E_\mu^{(+)}(\bar{x},t)|\{\alpha\}\rangle=\mathcal{E}_\mu(\{\alpha\},\bar{x},t)|\{\alpha\}\rangle \quad (7)$$

$$\langle\{\alpha\}|E_\mu^{(-)}(\bar{x},t)=\mathcal{E}_\mu(\{\alpha\},\bar{x},t)^*\langle\{\alpha\}|. \quad (8)$$

The integral in (6) is to be understood as a multiple integral over all α_k representing all modes k. If a corresponding mode expansion is made in (4), the two expressions (4) and (6) are brought into correspondence; the integrals over $P(\alpha)$ represent the ensemble average in (4), and the factors $\mathcal{E}_\mu^{(-)}(\{\alpha\},\bar{x}_i,t_i)\mathcal{E}_\mu^{(+)}(\{\alpha\},\bar{x}_i,t_i)$ are directly interpretable as the power (density) at the different times t_i. $P(\alpha)$ plays the role of a probability (except that it is not necessarily a positive quantity).[6]

Equation (4) is the basic formula needed to derive the spectrum of the photomultiplier anode current. In describing the photomultiplier, we assume that all photoelectrons produce in the anode circuit a current pulse of identical shape but fluctuating amplitude. The height of the individual current pulses fluctuates by virtue of the probabilistic nature of the secondary emission process. We assume that the bandwidth of the photomultiplier is much wider than the modulation bandwidth of the incident light, a condition that is satisfied in our experiments. If we denote the gain of the photomultiplier A, the electron charge e, the anode current I_0, then the spectrum of the anode current of the photomultiplier becomes[7] (see Appendix I)

$$\Phi(\omega)=A(eI_0/2\pi)\Gamma+Ae I_0\beta(\Phi_p(\omega)/\bar{p})=S_s+S_e. \quad (9)$$

[4] L. Mandel, Proc. Phys. Soc. (London) **72**, 1037 (1959).

[5] P. L. Kelley and W. H. Kleiner, Phys. Rev. **136**, A316 (1964).

[5a] R. J. Glauber, *Quantum Electronics and Optics* (*Les Houches Notes*) (Gordon and Breach, Science Publishers, Inc., New York, 1965).

[6] R. J. Glauber, Phys. Rev. Letters **10**, 84 (1963); Phys. Rev. **130**, 2529 (1963); **131**, 2766 (1963); *Quantum Electronics* (*Proceedings of the Third International Congress*), edited by N. Bloembergen and P. Grivet (Columbia University Press, New York, 1964), p. 111.

[7] This is a generalization of a formula derived by C. T. J. Alkemade, Physics **25**, 1145 (1959).

Here Γ is the shot-noise enhancement factor that is due to secondary emission; in general, it is less than 2, with $\Phi_p(\omega)$ the spectral density of the power $p(t)$:

$$\Phi_p(\omega)=\frac{1}{2\pi}\int_{-\infty}^{\infty}\langle p(t)p(t+\tau)\rangle_{\mathrm{av}}e^{-i\omega\tau}d\tau. \quad (10)$$

The first term in Eq. (9) is the enhanced shot noise of the photomultiplier. This term is present regardless of whether the light is modulated or not. The second term conveys information about the spectral density of $p(t)$, the power of the incident light. We shall use the symbol S_s for the shot-noise "background" and the symbol S_e for the "excess" noise produced by the time variation of the light power. An experimental determination of the second term, therefore, yields information about the time dependence of the incident light power.

Next, we consider the theory of the photoelectron counting experiment which provides another way of obtaining information about the fluctuation of the light power incident upon the photomultiplier. Denote the number of photoelectrons received within a time interval of duration T, by n. The mean-square deviation of the photoelectron count, averaged with respect to the compound Poisson distribution, and with respect to the statistics of the incoming light, follows from Eq. (4):

$$\langle n^2\rangle_{\mathrm{av}}-\bar{n}=\beta^2 2\int_t^{t+T}dt_2\int_t^{t_2}dt_1\langle p(t_1)p(t_2)\rangle_{\mathrm{av}}. \quad (11)$$

Introducing the new variable $\tau=t_2-t_1$ and assuming that the light statistics are stationary so that the correlation function $\langle p(t_1)p(t_2)\rangle_{\mathrm{av}}\equiv R_p(\tau)$ depends only on τ, one obtains

$$\langle n^2\rangle_{\mathrm{av}}-\bar{n}=\beta^2 2\int_0^T(T-\tau)R_p(\tau)d\tau. \quad (12)$$

By introducing a normalized correlation function $\rho_p(\tau)$ by

$$R_p(\tau)=\bar{p}^2[1+\rho_p(\tau)], \quad (13)$$

Eq. (12) can be written in the form

$$\langle n^2\rangle_{\mathrm{av}}-\bar{n}^2=\bar{n}+\frac{2\bar{n}^2}{T^2}\int_0^T(T-\tau)\rho_p(\tau)d\tau. \quad (14)$$

We have introduced the relationship between the average power $\bar{p}$ and the average count $\bar{n}$ in a time interval T

$$\bar{n}=\beta\bar{p}T. \quad (15)$$

The first term in Eq. (14) represents the Poisson value of the mean-square deviation of the photoelectron count that would result if the photosurface were illuminated by a light source of constant power (such as that produced by an ideal source of time-independent intensity). The second term contains the correlation function of the light power.

In the sequel we shall not plot the mean-square fluctuation, but rather the normalized second factorial moment defined by

$$F(2)=\frac{\langle\bar{n}(n-1)\rangle_{\mathrm{av}}-\bar{n}^2}{\bar{n}}=\frac{2\bar{n}}{T^2}\int_0^T(T-\tau)\rho_p(\tau)d\tau. \quad (16)$$

Note that the quantity $F(2)$ is zero if the power is time-independent, such as would be the case in an "ideal" laser with no amplitude fluctuations.

One may bring the equation for the spectral measurement into close correspondence with the measurement of $F(2)$ by noting that

$$R_p(\tau)=\int_{-\infty}^{\infty}e^{i\omega\tau}\Phi_p(\omega)d\omega. \quad (17)$$

The time-independent part of the correlation function $R_p(\tau)$ contributes a delta function to $\Phi_p(\omega)$. Defining by $\Phi_p{}^{ac}(\omega)$ that portion of $\Phi_p(\omega)$ which does not include the delta function at the origin, we obtain from Eq. (14),

$$F(2)=2\beta T\int_{-\infty}^{\infty}\frac{1-\cos\omega T}{(\omega T)^2}\frac{\Phi_p{}^{ac}(\omega)}{\bar{p}}d\omega. \quad (18)$$

Here we have taken into account that $\Phi_p{}^{ac}(\omega)$ is a symmetric function of ω. This equation establishes the connection between the measurement of $F(2)$ and the spectral measurement.

The counting experiment allows one to evaluate higher order factorial moments of the photoelectron count. According to Eq. (4), these enable one to find information on higher order correlation functions of the light power, an information that is not available from a simple spectral measurement. In the sequel we shall report measurements of normalized factorial moments of third and fourth order, defined by the general expression,

$$F(k)=\frac{\langle n(n-1)\cdots(n-k+1)\rangle_{\mathrm{av}}-\bar{n}^k}{\bar{n}^{(k-1)}}. \quad (19)$$

III. APPLICATION TO CAVITY LASER AMPLIFIER AND OSCILLATOR

We apply the equations developed for the spectral measurement and for the photoelectron counting to the case of a laser operating below and above threshold. We shall concentrate on a laser operating in a single mode of one single polarization. Below threshold this assumption is legitimate only if the laser is operated sufficiently near threshold. (See Sec. V.) In all of our experiments carried out above threshold, the laser operated in a single mode of one polarization.

A semiclassical analysis[8] of the laser oscillator driven by spontaneous emission noise gives the following re-

[8] H. A. Haus, J. Quantum Electron. 1, 179 (1965).

sult for the quantity $\Phi_p(\omega)/\bar{p}$ at $\omega\neq 0$:

$$\frac{\Phi_p(\omega)}{\bar{p}}=\frac{l}{\pi}\left|\frac{n_2/g_2}{(n_2/g_2)-(n_1/g_1)}\right|\times\frac{\hbar\omega_0}{Q_0|Q_m|}\frac{\omega_0^2}{\omega^2+(\omega_0/Q')^2}. \tag{20}$$

We have used the spectral density as a function of angular frequency, defined for both positive and negative frequencies. In (20) l is the loss of power between the laser output and the photomultiplier cathode; n_2 and n_1 are the populations of the upper and lower levels, respectively; g_2 and g_1 are their degeneracies; ω_0 is the resonance frequency of the cavity; (ω_0/Q_m) is the (usually negative) damping constant due to the maser material; Q_0 is the loaded Q of the "cold" cavity; that is, ω_0/Q_0 is the damping constant of the empty cavity in the absence of the maser material, or $\Delta\omega_0=\omega_0/Q_0$ is the bandwidth of the empty cavity; Q' is given by

$$\frac{1}{Q'}=\left|\frac{1}{Q_m^0}\right|-\frac{1}{Q_0}, \tag{21}$$

where Q_m^0 is the Q of the maser material obtained without the saturation caused by the optical field. Equation (20) is obtained directly from Eq. (11) of Ref. 8, except that here we use a spectral density expressed in angular frequency, allowing for both positive and negative frequencies, which is related to the spectrum $W_p(f)$ by a factor of 4π. Furthermore, the "hot" Q of the laser Q', above threshold is related to the power $\bar{p}$ emitted by the laser[9] by

$$\omega_0/Q'=(3\gamma/2G)\bar{p}, \tag{22}$$

where γ is a parameter of the equivalent Van der Pol circuit of the laser,[8] G is the loading conductance of the equivalent circuit of the laser, representing the loss of power to the outside space, and loading caused by internal losses (except for the loading or gain of the laser material) have been disregarded. The "hot" Q of the laser Q' is the quality factor that determines the rate at which amplitude disturbances relax to the steady state. This fact accounts for the appearance of Q' in the spectral bandwidth of the noise. The farther above threshold the laser operates, the stronger is the reaction to any disturbance and the faster the return to the steady state. From (22) and (20) we see that $1/Q'$, and thus the bandwidth of the spectrum $\Phi_p(\omega)$, is proportional to the output power $\bar{p}$ of the laser.

The same expression is obtained for the laser below threshold with one single mode and polarization except that Q_m in the denominator of Eq. (20) is replaced by Q_m^0, and the bandwidth of the spectrum is determined by a Q' given by

$$\frac{1}{Q'}=\frac{1}{Q_0}-\left|\frac{1}{Q_m^0}\right|. \tag{23}$$

[9] J. A. Mullen, Proc. IRE 48, 1467 (1960); see Eqs. (12) and (17).

Since $Q_m^0\simeq Q_m$ near threshold, henceforth we shall make no distinction between these two quantities. The power emitted by the laser below threshold is [Eq. (15) of Ref. 8] given by

$$\bar{p}=\left|\frac{n_2/g_2}{(n_2/g_2)-(n_1/g_1)}\right|\hbar\omega\frac{\omega_0}{Q_0}\frac{Q'}{|Q_m^0|}. \tag{24}$$

We see therefore that near threshold, where the variation in $|Q_m^0|$ may be disregarded, the hot Q, Q', is proportional to the power and thus the bandwidth of the excess noise, S_e of (9), is inversely proportional to the power.

The laser material becomes passive, when $n_2/g_2=n_1/g_1$. Equation (20) does not become singular in this case, as a perfunctory glance might indicate. Indeed, $|Q_m|$ becomes infinite at the same rate as $n_2/g_2-n_1/g_1$ approaches zero and thus no singularity occurs. This is obvious on physical grounds because the noise, caused by spontaneous transitions from the upper level to the lower level remains finite and the net Q of the cavity, at this point equal to the cold Q of the cavity, is finite also. When Eq. (20) is introduced into the spectral expression (9), one obtains for the ratio of excess noise to shot-noise

$$\frac{S_e}{S_s}=\frac{2\eta}{\Gamma}\left|\frac{n_2/g_2}{(n_2/g_2)-(n_1/g_1)}\right|\times\left(\frac{\Delta\omega_0}{\Delta\omega}\right)^2\frac{1}{1+\omega^2/\Delta\omega^2}, \tag{25}$$

where $\eta=l\varphi$ denotes the ratio of the rate of photoelectrons emitted by the photosurface of the photomultiplier to the rate of photons emitted by the laser. $\Delta\omega=\omega_0/Q'$ gives the width of the spectral curve, and $\Delta\omega_0=\omega_0/Q_0\simeq\omega_0(|Q_m|Q_0)^{1/2}$ is the bandwidth of the unexcited cavity. Equation (25) is the fundamental equation for the spectral measurement. It is valid near threshold, both below and above it provided only one mode contributes to the output. As threshold is approached from below, the $1/Q'$ of (23) decreases to zero, the bandwidth $\Delta\omega$ of the spectrum narrows and (25) becomes larger and larger. As threshold is passed, the bandwidth $\Delta\omega=\omega_0/Q'$ increases with increasing $|1/Q_m^0|$, i.e., increasing output power, and (25) decreases. When more than one mode contributes to the output, (25) does not hold. One may develop a simple relation to replace (25) for the case below threshold when all but one of the modes contributing to the output are broad-band. If only one linearly polarized mode is near threshold (we shall see that the Q_m for the observed narrow-band mode differs by less than 1% from Q_0) the others will be of much broader bandwidth and contribute mainly to the shot noise, but not to the excess noise term. For this case, when only a fraction f of the total emitted power is in the narrow-band mode, the ratio S_e/S_s decreases by a factor f^2

$$\frac{S_e}{S_s}=f^2\frac{2\eta}{\Gamma}\left|\frac{n_2/g_2}{(n_2/g_2)-(n_1/g_1)}\right|\times\left(\frac{\Delta\omega_0}{\Delta\omega}\right)^2\frac{1}{1+\omega^2/\Delta\omega^2}. \tag{26}$$

Equation (20), obtained from the Van der Pol theory of the laser, can also be applied to the counting experiment. In the counting experiment one needs the correlation function

$$\bar{p}^{-1}\langle p(t)p(t+\tau)\rangle_{\rm av}$$

which is the Fourier transform of (20). Again, one finds that both below and above threshold the following expression applies

$$F(2)=\frac{\langle n^2\rangle_{\rm av}-\bar{n}^2-\bar{n}}{\bar{n}}=2\eta\left|\frac{n_2/g_2}{(n_2/g_2)-(n_1/g_1)}\right| \times\left(\frac{\Delta\omega_0}{\Delta\omega}\right)^2\left[1-\frac{1}{\Delta\omega T}(1-e^{-\Delta\omega T})\right]. \quad (27)$$

As a function of the counting interval T, $F(2)$ increases linearly with T and then "saturates" at the value

$$2\eta\left|\frac{n_2/g_2}{(n_2/g_2)-(n_1/g_1)}\right|\left(\frac{\Delta\omega_0}{\Delta\omega}\right)^2.$$

Again one finds that in the case of one narrow-band mode carrying a fraction f of the total power and all remaining modes of much broader bandwidth, $F(2)$ is lowered by the factor f^2.

$$F(2)=f^2 2\eta\left|\frac{n_2/g_2}{(n_2/g_2)-(n_1/g_1)}\right|\left(\frac{\Delta\omega_0}{\Delta\omega}\right)^2 \times\left[1-\frac{1}{\Delta\omega T}(1-e^{-\Delta\omega T})\right]. \quad (28)$$

IV. THE HIGHER ORDER FACTORIAL MOMENTS

Below threshold the output of the laser has a Gaussian amplitude distribution of the electric field in each mode. The higher order correlation functions of random time functions with Gaussian amplitude distributions are all related to the lowest order correlation functions. Thus, for example, if x_1, x_2, x_3, and x_4 are Gaussian variables of zero mean, then

$$\langle x_1x_2x_3x_4\rangle_{\rm av}=\langle x_1x_2\rangle_{\rm av}\langle x_3x_4\rangle_{\rm av} +\langle x_1x_3\rangle_{\rm av}\langle x_2x_4\rangle_{\rm av}+\langle x_1x_4\rangle_{\rm av}\langle x_2x_3\rangle_{\rm av},$$

where all distinct pairs of indices are included in the summation, three in the present case.

The kth-order factorial moment of the photoelectron count within the time interval T contains the $(k-1)$th-order correlation function of the power. This in turn is related to the $(2k-1)$th-order correlation function of the amplitude. The third-order factorial moment contains averages of products of six Gaussian time functions, the fourth-order factorial moment contains averages of products of eight Gaussian variables. The former contains 15, the latter 105 terms. The algebra escalates rather rapidly. When more than one mode of the laser contributes to the output, the complications increase further. Simplifications occur when one may assume that all but one laser mode are broad-band. This situation is likely to be realized in the operation of a He-Ne laser near threshold where one mode near the maximum of the material linewidth predominates and, in general, one polarization is favored. We assume, therefore, that a fraction f of the total output of the laser is due to a narrow-band mode of one single polarization, and that the remaining power is attributable to modes of much wider bandwidths. All modes are assumed uncorrelated. With these assumptions, and under an assumed correlation function for the amplitude of the narrow-band "dominant" mode;

$$\langle a(t)a(t+\tau)\rangle_{\rm av}=\bar{a}^2e^{-\Delta\omega\tau/2} \quad (29)$$

one obtains for the normalized second factorial moment

$$F(2)=\frac{\langle n(n-1)\rangle_{\rm av}-\bar{n}^2}{\bar{n}} =f^2\frac{\bar{n}}{\Delta\omega T}2\left[1-\frac{1}{\Delta\omega T}(1-e^{-\Delta\omega T})\right]. \quad (30)$$

The above expression may be obtained directly from (14) for $f=1$, and $\rho_p(\tau)=\exp(-\Delta\omega\tau)$. Note that (30) agrees with (28). The only difference is that in (28) the Van der Pol theory has been used to obtain $\bar{n}$, whereas (30) applies to any Gaussian light.

The higher order factorial moments are obtained after lengthy algebra. The normalized third-order factorial moment is

$$F(3)=\frac{\langle n(n-1)(n-2)\rangle_{\rm av}-\bar{n}^3}{\bar{n}^2}=3F(2) +f^3\frac{\bar{n}}{\Delta\omega T}3!\frac{2}{\Delta\omega T}\left[(1+e^{-\Delta\omega T})-\frac{2}{\Delta\omega T}(1-e^{-\Delta\omega T})\right] \quad (31)$$

and the normalized fourth-order factorial moment is

$$F(4)=\frac{\langle n(n-1)(n-2)(n-3)\rangle_{\rm av}-\bar{n}^4}{\bar{n}^3}=4F(3)-6F(2) +f^4\frac{\bar{n}}{\Delta\omega T}3!\frac{2}{\Delta\omega T}\left[1+\frac{8}{\Delta\omega T}-\frac{28}{(\Delta\omega T)^2} +\left(4+\frac{22}{\Delta\omega T}+\frac{26}{(\Delta\omega T)^2}\right)e^{-\Delta\omega T}+\frac{2}{(\Delta\omega T)^2}e^{-2\Delta\omega T}\right]. \quad (32)$$

Thus far we have been concerned with the factorial moments below threshold. The factorial moments above threshold assume a much simpler form when the number n of photoelectrons emitted by the illuminated photosurface within a time interval T differs only little

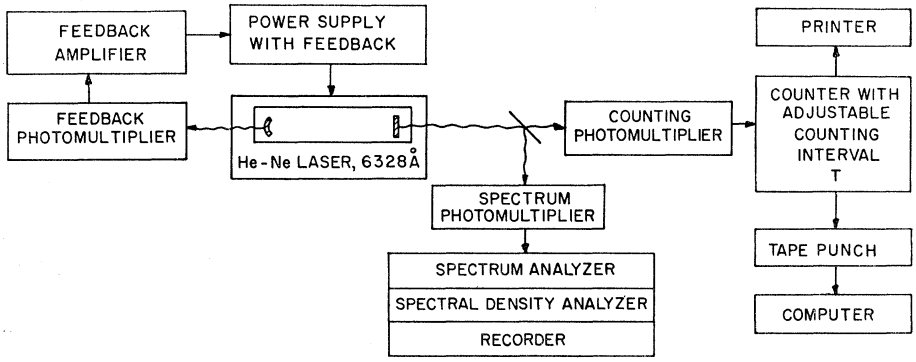

FIG. 1. Experimental arrangement.

from the average value $\bar{n}$. If this is so, all higher order factorial moments of n can be expressed in terms of the second-order factorial moment. As an example, consider the third-order moment

$$\langle n(n-1)(n-2)\rangle_{\rm av}-\bar{n}^3=\langle n^3\rangle_{\rm av}-3\langle n^2\rangle_{\rm av}+2\bar{n}-\bar{n}^3. \quad (33)$$

Setting $n=\bar{n}+\Delta n$, with $\langle\Delta n\rangle_{\rm av}=0$, we have

$$\langle n^2\rangle_{\rm av}=\bar{n}^2+\langle\Delta n^2\rangle_{\rm av} \quad (34)$$

and

$$\langle n^3\rangle_{\rm av}=\bar{n}^3+3\bar{n}\langle\Delta n^2\rangle_{\rm av}+\langle\Delta n^3\rangle_{\rm av}. \quad (35)$$

Introducing (35) into the factorial moment and disregarding $\bar{n}$, $\langle\Delta n^2\rangle_{\rm av}$, and $\langle\Delta n^3\rangle_{\rm av}$, compared with $\bar{n}\langle\Delta n^2\rangle_{\rm av}$, one has

$$F(3)=\frac{\langle n(n-1)(n-2)\rangle_{\rm av}-\bar{n}^3}{\bar{n}^2}$$

$$\cong\frac{3(\langle\Delta n^2\rangle_{\rm av}-\bar{n})}{\bar{n}}=3F(2). \quad (36)$$

In a similar way we find for the normalized fourth-order factorial moment

$$F(4)=\frac{\langle n(n-1)(n-2)(n-3)\rangle_{\rm av}-\bar{n}^4}{\bar{n}^3}$$

$$\cong 6F(2)\cong 2F(3). \quad (37)$$

Note that a certain similarity exists between (36), (37), and (31), (32). For $f\to 0$, the two expressions become identical. This is to be expected because the power carried by a narrow-band mode with a large admixture of broad-band modes is similar to steady power with a small modulation.

Furthermore, note that it is difficult to detect properties other than those of the second-order moment $\langle\Delta n^2\rangle_{\rm av}$ from a measurement of the higher factorial moments of n produced by a laser above threshold. The terms that were disregarded in the numerator of $F(4)$ are of the order of $\langle\Delta n^4\rangle_{\rm av}$ which, if Δn is near to a Gaussian, would be of the order of $\bar{n}^2$. The terms retained are of the order of $\bar{n}^3$. Thus, the error is $1/\bar{n}$, a very small quantity in our measurements. This quantity, in fact, lies within the experimental fluctuations (see Sec. V).

V. EXPERIMENTS

The experimental arrangement is shown in Fig. 1. An internal mirror laser of nearly hemispherical geometry with a mirror spacing of 49.2 cm was used. The i.d. of the quartz tube was 3.9 mm. The laser was dc excited and operated at 6328 Å. When appreciable gas discharge fluctuations were noticed occasionally, they were suppressed by optimizing the external circuitry and by positioning a magnet near the discharge. The laser was stabilized to less than 1% long-term drift in intensity by a feedback circuit with a time constant of approximately 1/50 of a second. The feedback circuit sensed the light emerging from the mirror of 50-cm radius with a reflectivity of 99.9%. The light through the flat mirror with a reflectivity of 99% was fed partly to one photomultiplier connected to a counter and partly to a second photomultiplier connected to spectrum analyzing equipment. The counter measured the number of photoelectrons within a sequence of preset time intervals of adjustable duration T. In the experiments T was varied from 10^{-6} to 10^{-1} sec. The counts were recorded on tape which could be fed directly to a computer. The computer evaluated the normalized factorial moments $F(2)$, $F(3)$, and $F(4)$ as defined by (19).

Simultaneously with the counting data, spectral data were obtained. The spectrum was studied in the 0–17-Mc/sec range. Different spectrum analyzers were used for different ranges of the frequency spectrum. Scanning velocities were varied from 0 to 4 cps/sec at the low-frequency end, to 10 to 1000 cps/sec in the high-frequency range of the spectrum. The corresponding intermediate-frequency bandwidths ranged from a minimum of 10 cps to a maximum of 10 000 cps. The spectrum analyzer output was fed into a spectral density analyzer, with integration times of 1 or 5 sec, and then to a chart recorder. The spectral data were always checked against the response obtained from a broad-band (tungsten filament) light source. The experimental results obtained from the spectrum measurement are shown in Fig. 2. The curves are labeled by their cor-

responding photoelectron emission rates $\bar{n}$ (in sec^{-1}) of the photocathode. Above threshold, 7 of the 12 dynodes of the photomultiplier were shorted to the anode. Lorentzian curves could be fitted with very good accuracy onto all curves above threshold and to the top curves below threshold. At all power levels of Fig. 2, the laser operated stably and reproducibly for several months. The small modulation spike at approximately 170 kc/sec both above and below threshold is due to residual discharge oscillations. The following quantitative predictions can be made from the theoretical

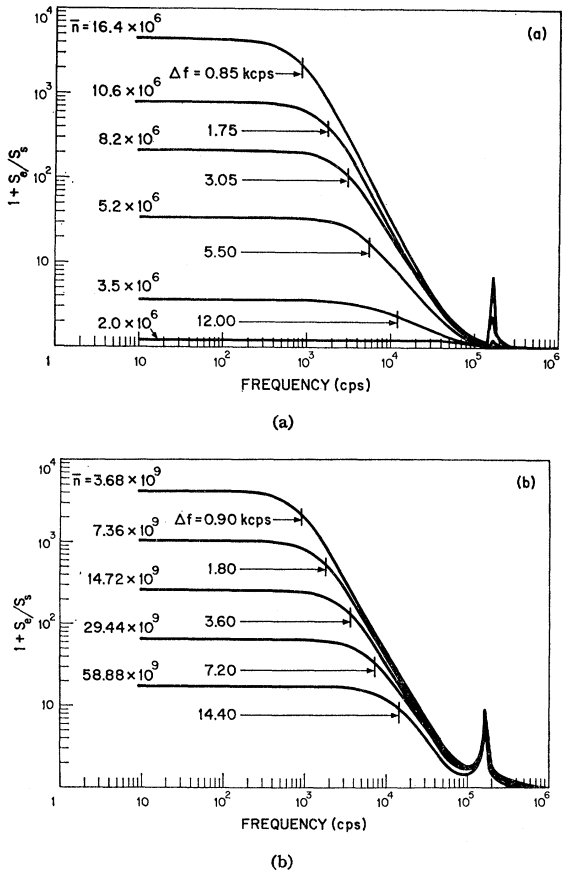

FIG. 2. Observed photomultiplier current spectra. (a) Below-threshold operation; (b) above-threshold operation.

formulas (22), (24), and (25), and compared with experiment:

(1) The bandwidth of the "excess noise" spectrum is inversely proportional to the laser power $\bar{p}$ below threshold, and proportional to $\bar{p}$ above the threshold. Deviation from the $1/\bar{p}$ dependence occurs only below threshold when more than one linearly polarized mode contributes to the output. In Fig. 3 we plot the experimentally obtained bandwidths as a function of power. The theoretical $\bar{p}$ dependence above threshold is shown by a solid line. The below threshold data may be compared with a $1/\bar{p}$ dependence shown by a solid line and

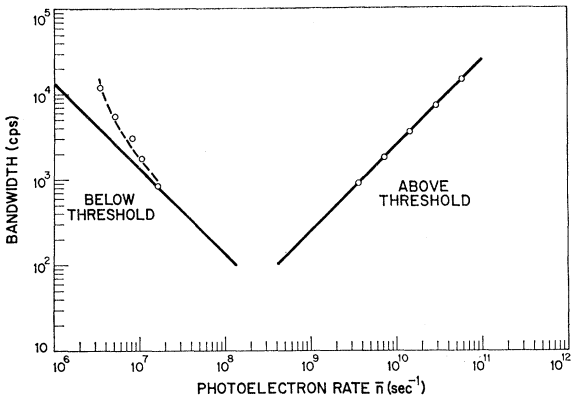

FIG. 3. Bandwidth versus laser power.

with another plot shown by a dashed curve obtained under the assumption that 2.5×10^6 (sec^{-1}) photoelectrons were due to other than the dominant narrow-band mode. The observed approximately linear polarization of the $\bar{n}=1.64\times10^7$ sec^{-1} curve is an indication that the contribution of the "background" power was relatively weak at this power level. At lower powers the polarization became more and more isotropic. The "background" power, in fact, cannot be expected to stay independent of the excitation in our experiment. The "dashed" curve is shown only to indicate that the bandwidth data are matched better by assuming that other than the dominant mode contribute to the output power.

(2) The ratio S_e/S_s near 0 frequency is inversely proportional to the square of the bandwidth, and therefore directly proportional to the square of the laser power below threshold and inversely proportional to the square of the laser power above threshold. In Fig. 4 we show the observed S_e/S_s near zero frequency as a function of power. The $1/\bar{p}^2$ dependence above threshold and $\bar{p}^2$ dependence below threshold are shown by solid lines, while the dashed curve for below threshold is obtained under the assumption that 2.5×10^6 sec^{-1}

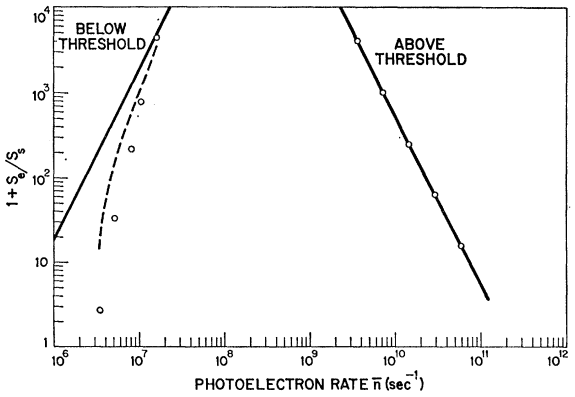

FIG. 4. Ratio of excess noise to shot-noise versus laser power.

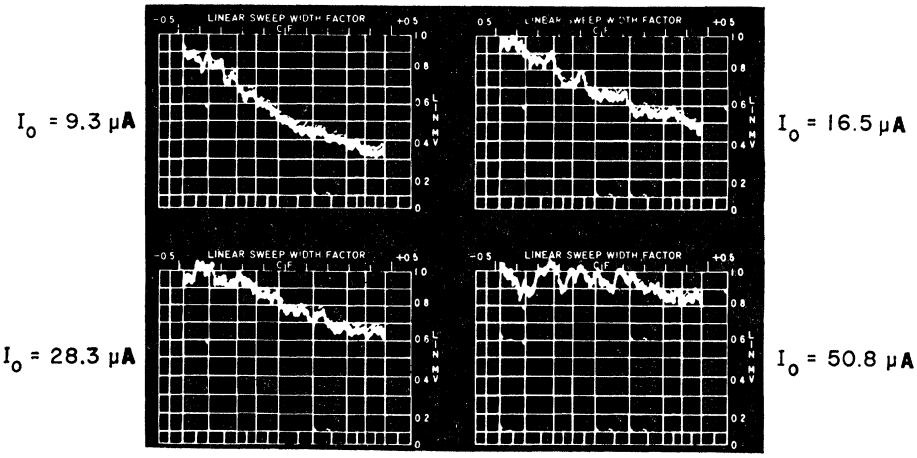

FIG. 5. Photomultiplier current spectra above threshold. Anode current: 9.3, 16.5, 28.3, 50.8 μA; sweep width: 0–5 kc/sec.

photoelectrons are due to broad-band background. The comments made in connection with Fig. 3 apply here too.

(3) The measured ratio S_e/S_s from the $\bar{n}=3.68\times10^9$ $\sec^{-1}$ curve above threshold yields $(n_2/g_2)/[(n_2/g_2)-(n_1/g_1)]=1.97$, by using (25), the measured values of $\eta=4.9\times10^{-3}$, $\Gamma=1.3$, and taking $\Delta\omega_0=2\pi\times4.7\times10^5$ cps as computed from the transmittance of the mirrors.

(4) From (25) one finds that the ratio S_e/S_s above and below threshold is the same for curves of equal bandwidth if, below threshold, one linearly polarized mode predominates, as is the case for the $\bar{n}=1.64\times10^7$ curve. The two top curves in Figs. 2(a) and 2(b) have comparable bandwidths. If one predicts, using (25), from the above threshold curves the ratio S_e/S_s below threshold for the 1.64×10^7 $\sec^{-1}$ curve, taking into account the difference in bandwidths, one finds $S_e/S_s=4600$, which should be compared with the measured value of 4400.

(5) From (24) one may predict the photon emission rate from the laser, assuming the value $(n_2/g_2)/[(n_2/g_2)-(n_1/g_1)]=1.97$; using the bandwidth corresponding to the curve $\bar{n}=1.64\times10^7$ $\sec^{-1}$ one predicts for it a photon rate of 3.22×10^9 $\sec^{-1}$. The measured rate was 3.34×10^9 $\sec^{-1}$. Note that the agreement of the predicted value of the photon rate with the experimentally obtained value confirms our assumption that the noise is due to spontaneous emission.

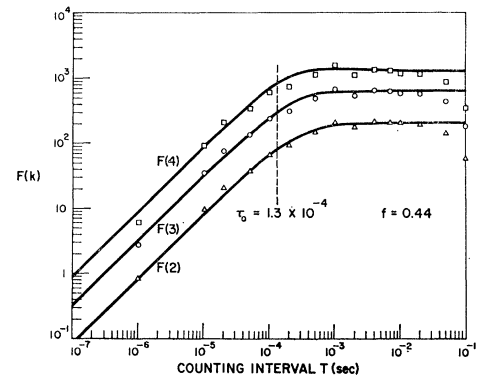

FIG. 6. Normalized factorial moments below threshold (photon rate 2.82×10^9 $\sec^{-1}$, photoelectron rate 4.31×10^6 $\sec^{-1}$).

Thus the measurements of S_e/S_s, bandwidth, and power are in reasonable agreement with the theoretically predicted values. If one does not care about integrating the spectral measurements over appreciable lengths of time, one may observe quite vividly the change in bandwidth as a function of laser power. Figure 5 shows a set of spectra observed on the spectrum analyzer with a 10-sec full sweep for the laser operating above threshold. All curves were adjusted to a common maximum of unity (full scale deflection).

Next, we turn to the counting experiments. Equations (30), (31), and (32) for the normalized factorial moments for below threshold operation are compared with an experimental run in Fig. 6. This run is sufficiently below threshold so that the theory, in which a Gaussian amplitude distribution of the light is assumed, can be used. The theoretical curve for the second-order factorial moment $F(2)$ was matched to the experimental points by adjusting f and $\Delta\omega$. Using the values $f=0.44$ and $\tau_0=1/\Delta\omega=1.3\times10^{-4}$, we plotted the theoretical curves for $F(3)$ and $F(4)$. The agreement with the experimental points is seen to be good up to $T=2\times10^{-2}$ sec. For longer counting intervals we find that the experimental points fall below the theoretical curve. This is due to the influence of the feedback network which had a time constant of the order of 2×10^{-2} sec.

Above threshold operation of the laser occurred in one single mode. If one assumes that the field amplitude of the laser is of the form

$$a(t)=[a_0+a_1(t)]\cos(\omega_0T+\varphi),$$

where

$$|a_1|\ll a_0$$

and

$$\langle a_1(t)a_1(t+\tau)\rangle_{\mathrm{av}}/\langle a_1^2\rangle_{\mathrm{av}}=e^{-\Delta\omega|\tau|},$$

one obtains for the normalized second-order factorial

moment

$$F(2)=\frac{\langle n(n-1)\rangle_{\rm av}-\bar{n}^2}{\bar{n}}$$

$$\cong 8m^2\frac{\bar{n}}{\Delta\omega T}\left[1-\frac{1}{\Delta\omega T}(1-e^{-\Delta\omega T})\right]. \quad (38)$$

Equation (38) is very similar to the result for below-threshold operation, except that the modulation coefficient, $m^2=\langle|a_1|^2\rangle_{\rm av}/a_0^2$, appears as a multiplier. If, indeed, the fluctuation amplitude a_i is small compared with the steady-state amplitude, the higher order factorial moments are dominated by the mean-square fluctuation $\langle n^2\rangle_{\rm av}-\bar{n}^2$, and all of the higher order moments can be related to $F(2)$, as we indicated in Sec. IV.

A typical result of an experimental run above threshold is shown in Fig. 7. Because of the small fluctuation amplitude a_1, we found that the feedback network had greater influence than below threshold. The deviation from the theoretical T dependence of (27) occurred already at counting intervals T of the order of 5×10^{-3}. The solid curves for $F(3)$ and $F(4)$ were obtained by multiplying the curve for $F(2)$ by 3 and 6, respectively. This was done in accordance with the theoretical predictions of Eqs. (36) and (37). It will be observed that the agreement is quite good.

An interesting difference may be noted between Figs. 6 and 7. The spacings between the straight-line asymptotes in the two figures are distinctly different in agreement with the prediction of the equations of Sec. IV. This difference provides one possible way for distinguishing between below threshold and above threshold operation.

As mentioned previously, a measurement of the spectrum contains the same information as a measurement of $F(2)$. Figure 8 shows a comparison of the two types of experiments. An experimentally obtained current spectrum obtained below threshold is shown. The function $F(2)$ versus T is predicted from the spectrum by using (9), (18), (26), and (27). The solid curve gives $F(2)$

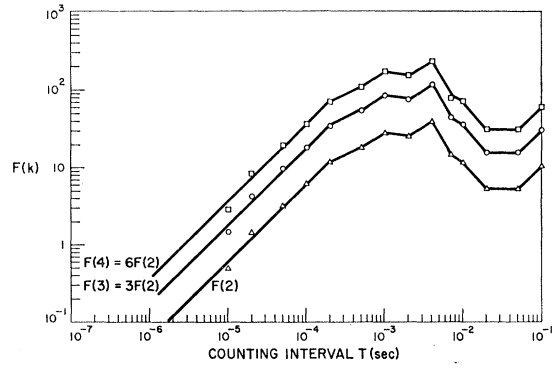

FIG. 7. Normalized factorial moments above threshold (photon rate 8.15×10^{11} sec^{-1}, photoelectron rate 11.09×10^6 sec^{-1}).

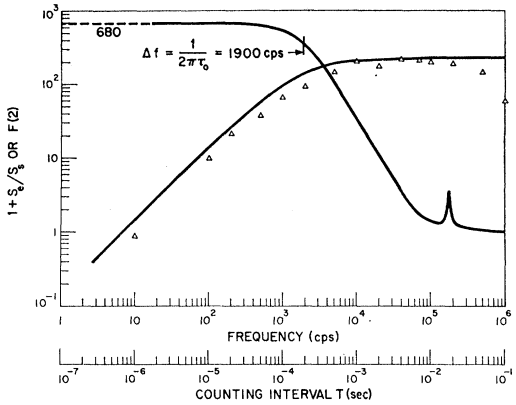

FIG. 8. Comparison of the spectrum measurement with normalized second factorial moment.

predicted from the spectrum measurement and the experimentally obtained points are shown. The agreement is seen to be reasonable.

VI. CONCLUSIONS

The experiments presented here have shown that the amplitude noise of an optical maser is mainly caused by spontaneous emission when the laser is operated near threshold (see point 5 of Sec. V). This finding should be contrasted with experiments on the phase or frequency noise of an optical maser reported by Jaseja *et al.*[10] Even in the best possible vibration-free surroundings, it was found that the linewidth of the laser was considerably wider than that predicted under the assumption that spontaneous emission noise is solely responsible for the frequency noise. Our experiments tend to show that with suitable care, vibrations of the mirrors which were mainly responsible for the frequency noise observed by Jaseja *et al.*, did not affect appreciably the amplitude noise. In other words, the frequency-to-amplitude conversion was sufficiently low so that the effect of the spontaneous emission noise on the amplitude fluctuations could be observed in spite of residual mirror vibrations and other causes of frequency noise.

The experiments reported here bear some resemblance to the Hanbury Brown and Twiss correlation experiments[11] and coincidence counting experiments.[12]

An analysis[13] similar to the one made by Hanbury Brown and Twiss shows that the signal-to-noise ratio of the spectrum measurement for a Gaussian amplitude distribution of the incident light of bandwidth $\Delta\omega$ is

$$(\text{signal/noise})|_{\rm spectrum}=(2\bar{r}/\Gamma\Delta\omega)(BT_0)^{1/2}, \quad (39)$$

where $\bar{r}=I_0/Ae$ is the photoelectron emission rate.

[10] T. S. Jaseja, A. Javan and C. H. Townes, Phys. Rev. Letters **10**, 165 (1963).
[11] R. Hanbury Brown and R. Q. Twiss, Proc. Roy. Soc. (London) A242, 300 (1957).
[12] G. A. Rebka and R. V. Pound, Nature **180**, 1035 (1957).
[13] H. A. Haus, MIT Research Laboratory of Electronics Internal Memorandum No. 170, 1965 (unpublished).

In the spectral measurement signal is defined by S_0 (near zero frequency), and the noise is defined as the experimental uncertainty in the determination of the shot-noise level by the equipment of finite bandwidth B and finite integration time T_0. The experimental uncertainty, in turn, is computed as the rms deviation of the experimental value of the shot-noise level from the ideal value for a true Poisson process.

A very similar expression is obtained for the signal-to-noise ratio for the experimental determination of $F(2)$ in the counting measurements. In this case signal is defined as the ideal value of $F(2)$ obtained from an ensemble average over infinite number of samples. The noise is defined in turn as the rms deviation of $F(2)$ for a Poisson process with the ensemble average replaced by an average over N samples. Again, under the same assumptions about the incident light, we have

$$(\text{signal/noise})\,|_{\text{count}}=(\sqrt{2}\bar{r}/\Delta\omega)\sqrt{N}\,, \qquad (40)$$

where N is the number of samples taken. Both expressions for the signal-to-noise ratio predict an accuracy comparable to that obtainable in the Hanbury Brown and Twiss correlation measurement and coincidence counting experiment. In order to obtain information about the spectral shape of the incident light power, it is necessary in the Hanbury Brown and Twiss experiment to introduce delays which are of the order of the inverse bandwidth of the light to be detected. In the present experiment this would call for delays of the order of milliseconds, a delay that is difficult to achieve. The spectral measurement and the counting experiment reported here are convenient ways of measuring the spectrum or correlation functions of narrow-band light.

To obtain an impression of the signal-to-noise ratio achievable in the present experiment, consider Fig. 6, with $r=4.31\times10^6$, $\Delta\omega=1/\tau_0=0.77\times10^4$, and $N\approx250$. One obtains from (40), signal/noise$=1.25\times10^4$. The deviation of points from the smooth curve in Fig. 6 is larger than predicted by this expression. The scatter is most likely due to the slight changes in the laser operating point during the measurement, since the feedback signal was derived from a high-gain photomultiplier under normal laboratory (instead of highly temperature-stabilized) environment.

ACKNOWLEDGMENTS

The authors gratefully acknowledge many helpful discussions with Dr. A. Javan, Dr. P. L. Kelley, Dr. W. H. Kleiner, Dr. M. M. Litvak, and Dr. A. Szöke. They are especially grateful to Dr. Kelley who read the manuscript and made many helpful suggestions, and to P. Trent for the computer programming.

APPENDIX I: CORRELATION FUNCTION OF PHOTOEMISSION CURRENT

We derive the correlation function of the current flowing in the anode of a photomultiplier irradiated by light whose power level depends upon time. The derivation follows that of Davenport and Root[14], but deviates from it insofar as the assumed probability of emission of a photoelectron from the photocathode is a function of time and that the current pulses in the anode are of varying height. The time function of the anode current can be written as

$$f_T(t)=\textstyle\sum_k i(t-t_k)\,. \qquad (I1)$$

The respectively time-shifted functions $i(t-t_k)$ represent the current pulses induced in the anode circuit due to a photoelectron from the photocathode. They are of varying height and shape, because of the statistical nature of the secondary emission process. The average over the statistics of the secondary emission process gives

$$\int_{-\infty}^{\infty}\bar{i}(t-t_k)dt=eA\,, \qquad (I2)$$

where e is the electron charge and A is the photomultiplier gain. The summation in (I1) is carried over all current pulses occurring within a specified time interval. We choose for the time interval, a period extending from $t=-T/2$ to $t=T/2$. (Because the incident light flux is assumed to be time-dependent, the choice of the origin for the time interval will affect the probability distribution of emission. Eventually the time interval will be made to approach infinity; thus, the choice of the time origin becomes unimportant.) We define the function

$$R(T,\tau)=\langle f_T(t)f_T(t+\tau)\rangle_{\text{av}}\,. \qquad (I3)$$

Equation (I3) indicates an ensemble average obtained from an ensemble of wave forms of length T. One may envisage the ensemble to be generated by the output of many identical photomultipliers, all of which are illuminated by light with the same power variations with respect to time.

The ensemble average is obtained in four steps. First, one singles out all the samples that have exactly K current pulses emitted within the time T. [In doing so one disregards those samples in which $i(t-t_j)$ lies partly inside and partly outside the time interval $-T/2\leqslant t\leqslant T/2$, an approximation that is legitimate as long as T is sufficiently long.] The probability of finding the ith current pulse within the time increment t_i, t_i+dt_i is

$$p(t_i)dt_i\Big/\int_{-T/2}^{T/2}p(t_i)dt_i=r(t_i)dt_i\,. \qquad (I4)$$

[14] W. B. Davenport Jr., and W. L. Root, *Random Signals and Noise* (McGraw-Hill Book Company, Inc., New York, 1958), Sec. 7-4.

Thus, averaging over all these samples, one obtains

$$R(T,\tau)=\int_{-T/2}^{T/2}\cdots\int_{-T/2}^{T/2}\sum_{k=1}^{K} i(t-t_k)\times\sum_{j=1}^{K} i(t-t_j+\tau)r(t_1)\cdots r(t_K)dt_1\cdots dt_K. \quad (I5)$$

The product of the two summations in Eq. (I5) can be written as a double summation of K^2 terms. Within this summation there are K^2-K terms containing the integral, $i(t-t_k)i(t-t_j+\tau)$ pertaining to unequal time instants t_k and t_j, and K terms with the same pulse arrival time t_K occurring in both factors. All terms in the double summation corresponding to two different current pulses can be integrated as follows

$$\int_{-T/2}^{T/2}\cdots\int_{-T/2}^{T/2} i(t-t_k)i(t-t_j+\tau)\times r(t_1)\cdots r(t_K)dt_1\cdots dt_K=\int_{-T/2}^{T/2}\int_{-T/2}^{T/2} i(t-t_k)\times i(t-t_j+\tau)r(t_k)r(t_j)dt_k dt_j. \quad (I6)$$

Those terms corresponding to the same photoelectron integrate to

$$\int_{-T/2}^{T/2}\cdots\int_{-T/2}^{T/2} i(t-t_j)i(t-t_j+\tau)r(t_1)\cdots r(t_K)\times dt_1\cdots dt_K=\int_{-T/2}^{T/2} i(t-t_j)i(t-t_j+\tau)r(t_j)dt_j. \quad (I7)$$

Second, one considers the average over the number of current pulses received within the time interval T. One makes use of Eq. (I4), and the relations

$$\sum_{K=1}^{\infty} W(K)K=\sum_{K=1}^{\infty}\frac{\bar{n}^K}{K!}e^{-\bar{n}}K=\bar{n}, \quad (I8)$$

$$\sum_{K=1}^{\infty} W(K)(K^2-K)=\bar{n}^2, \quad (I9)$$

where

$$\bar{n}=\beta\int_{-T/2}^{T/2} p(t)dt \quad (I10)$$

is the average number of photoelectrons emitted within the time interval T from the photocathode. With these expressions, the function $R(T,\tau)$ of Eq. (I5) can be written in the form

$$R(T,\tau)=\beta^2\int_{-T/2}^{T/2}\int_{-T/2}^{T/2} dt_k dt_j p(t_k)\times p(t_j)i(t-t_k)i(t-t_j+\tau)+\beta\int_{-T/2}^{T/2} dt_k p(t_k)\times i(t-t_k)i(t-t_k+\tau). \quad (I11)$$

The third step takes into account the generally statistical character of the variations of the incident light intensity. The previous ensemble of photomultipliers all illuminated by light with identical time variations may now be considered to be one subensemble of the ensemble representing the light statistics. Each subensemble in the over-all ensemble corresponds to a particular time function of the light intensity. One takes an additional average of Eq. (I11) with respect to the statistics of the incident light:

$$\langle p(t_k)\rangle_{\text{av}}=\bar{p}, \text{ the average power}, \quad (I12)$$

and

$$\langle p(t_k)p(t_j)\rangle_{\text{av}}=R_p(t_k-t_j), \quad (I13)$$

where $R_p(t_k-t_j)$ is the autocorrelation function of the light power. We obtain for Eq. (I11)

$$R(T,\tau)=\beta^2\int_{-T/2}^{T/2}\int_{-T/2}^{T/2} dt_k dt_j R_p(t_k-t_j)i(t-t_k)\times i(t-t_j+\tau)+\beta\bar{p}\int_{-T/2}^{T/2} dt_k i(t-t_k)i(t-t_k+\tau). \quad (I14)$$

The autocorrelation function of the photomultiplier anode current is obtained by letting T approach infinity.

As a fourth step, we take an average with respect to the statistics of the secondary emission process. We define the autocorrelation function of a current pulse at the time t_k:

$$R_{kk}(\tau)=\lim_{T\to\infty}\int_{-T/2}^{T/2} dt_k\langle i(t-t_k)i(t-t_k+\tau)\rangle_{\text{av}} \quad (I15)$$

and the cross correlation function between pulses occurring at different times:

$$R_{kj}(t_k-t_j+\tau)=\lim_{T\to\infty}\int_{-T/2}^{T/2} dt\langle i(t-t_k)i(t-t_j+\tau)\rangle_{\text{av}}. \quad (I16)$$

Introducing these definitions and the new variable $\sigma=t_k-t_j$ into (I14), we finally obtain in the limit $T\to\infty$

$$R(\tau)=\lim_{T\to\infty} R(T,\tau)=\beta^2\int_{-\infty}^{\infty} d\sigma R_p(\sigma)R_{kj}(\sigma+\tau)+\beta\bar{p}R_{kk}(\tau). \quad (I17)$$

The Fourier transform of (I17) gives the spectrum $\Phi(\omega)$ of the photomultiplier anode current

$$\Phi(\omega)=2\pi\beta^2\Phi_{kj}(\omega)\Phi_p(\omega)+\beta\bar{p}\Phi_{kk}(\omega).$$

In the case in which all anode current pulses may be

treated as delta functions of varying area qA,

$$i(t-t_k)=qA\,\delta(t-t_k), \tag{I18}$$

where q is the charge content of the pulse referred to the first dynode of the photomultiplier, so that $\bar{q}=e$, and A is the gain, one obtains for (I17)

$$\Phi(\omega)=\beta^2e^2A^2\Phi_p(\omega)+\Gamma(\beta\bar{p}e^2A^2/2\pi). \tag{I19}$$

where $\Gamma=\langle q^2\rangle_{\rm av}/\bar{q}^2$. Noting that the anode current is given by

$$I_0=Ae\beta\bar{p}, \tag{I20}$$

one can rewrite Eq. (I19) as

$$\Phi(\omega)=I_0(Ae/2\pi)[\Gamma+2\pi\beta\Phi_p(\omega)/\bar{p}]. \tag{I21}$$

PHYSICAL REVIEW VOLUME 141, NUMBER 1 JANUARY 1966

Optical Nonlinearities of a Plasma*

N. BLOEMBERGEN† AND Y. R. SHEN
Department of Physics, University of California, Berkeley, California
(Received 6 August 1965)

Second-harmonic generation and stimulated Raman effects for a plasma are calculated by the same methods that have been used for bound electrons. The nonlinear susceptibility describing the stimulated Raman effect in a gaseous or metallic plasma is 6 to 10 orders of magnitude smaller than the corresponding effect in liquids. This process in a plasma can also be described as the parametric interaction between a damped plasma wave and two light waves. The second-harmonic generation from a plasma boundary is dominated by a surface term which originates from the discontinuity in the normal component of the electric field. It is shown that the observed second-harmonic generation from metallic silver probably stems from bound ion cores in the surface layer rather than from a plasma surface term.

I. INTRODUCTION

THE basic nonlinearity in the interaction between a free electron and an electromagnetic wave is caused by the Lorentz force. Additional nonlinearities may result from convective density fluctuations in the plasma. The nonlinearities in gaseous plasmas have been studied extensively in the microwave region of the electromagnetic spectrum.[1,2] Recently much attention has been given to optical nonlinearities of a plasma, although they are by their very nature rather small.[3–11] In this paper hydrodynamic terms and convection will be ignored.

The same basic formalism can be used to describe the nonlinearities for bound and free electrons. This is particularly evident in the formulation of Cheng and Miller[5] and of Pine,[12] who emphasized the self-consistent-field description of the nonlinear susceptibilities. In Sec. II of this paper, the second-harmonic volume polarization for a plasma is rederived. The self-consistent-field correction on this longitudinal polarization is explicitly exhibited in the same manner as has been done by Ehrenreich and Cohen[13] for the longitudinal linear dielectric constant. In Sec. III, it is shown that surface terms are actually more important than the volume effect for the second-harmonic generation (SHG) from a metallic surface. Jha[14] has first called attention to these plasma surface terms. Our results are somewhat different from Jha's and in better agreement with recent experimental observations. We show furthermore that the dominant contribution to the SHG may come from bound electrons in the ion cores at the surface rather than from the conduction electrons.

The next higher order nonlinearity describes the Raman-type effects in a plasma. If, for example, a laser beam at frequency ω_L is incident on a plasma, the plasma will present exponential gain for a light beam

* This research was supported by the U. S. Office of Naval Research. An abbreviated version of this work was presented at the Physics of Quantum Electronics Conference, Puerto Rico, 1965 (unpublished).
† On leave from Harvard University.
[1] P. A. Sturrock, Thermonucl. Res. (GB) **2**, 158 (1961).
[2] R. F. Whitmer and E. B. Barrett, Phys. Rev. **121**, 661 (1961); *ibid.* **125**, 1478 (1962).
[3] N. Bloembergen, Proc. IEEE **51**, 124 (1963).
[4] R. Kronig and J. I. Boukema, Proc. Koninkl. Ned. Akad. Wetenschap. **66B**, 8 (1963).
[5] H. Cheng and P. B. Miller, Phys. Rev. **134**, A683 (1964).
[6] P. M. Platzman, S. J. Buchsbaum, and N. Tzoar, Phys. Rev. Letters **12**, 573 (1964); P. M. Platzman and N. Tzoar, Phys. Rev. **136**, A11 (1964).
[7] D. F. Dubois and V. Gilinsky, Phys. Rev. **135**, A995 (1964).
[8] N. Kroll, A. Ron, and N. Rostoker, Phys. Rev. Letters **13**, 83 (1964).
[9] H. Cheng and Y. C. Lee, Phys. Rev. Letters **14**, 426 (1965).
[10] D. F. Dubois, Phys. Rev. Letters **14**, 818 (1965).
[11] Various authors in *Proceedings of the Conference on the Physics of Quantum Electronics, Puerto Rico* (McGraw-Hill Book Company, Inc., New York, 1965).
[12] A. Pine, Phys. Rev. **139**, A901 (1965). The authors are indebted to Dr. Pine for making his manuscript available before publication.
[13] H. Ehrenreich and M. H. Cohen, Phys. Rev. **115**, 786 (1959).
[14] S. S. Jha, Phys. Rev. **140**, A2020 (1965). The authors are indebted to Dr. Jha for receiving a copy of this paper prior to publication.

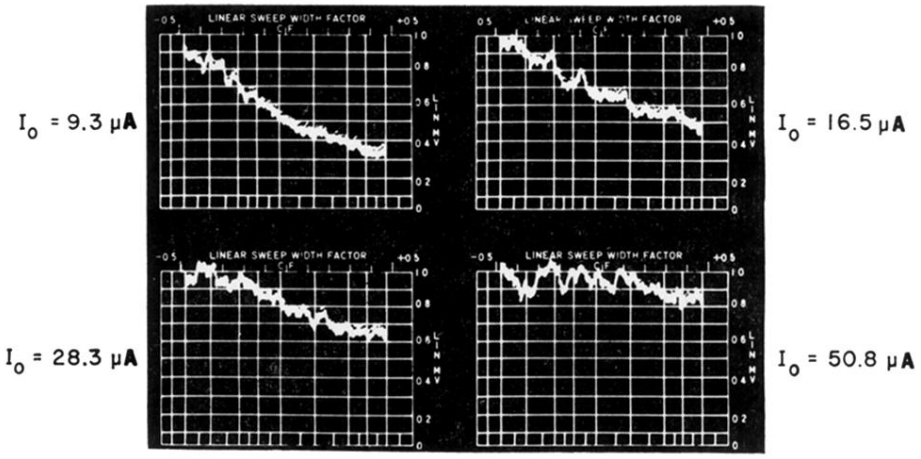

FIG. 5. Photomultiplier current spectra above threshold. Anode current: 9.3, 16.5, 28.3, 50.8 μA; sweep width: 0–5 kc/sec.